High-frequency magnetic response of crystalline and nanocrystalline antiferromagnetic NiO

Kacper Brzuszek,[1] Caroline A. Ross,[2] and Andrzej Janutka[1]
[1)]*Department of Theoretical Physics, Wroclaw University of Science and Technology, 50-370 Wrocław, Poland*
[2)]*Department of Materials Science and Engineering, Massachusetts Institute of Technology, Cambridge, Massachusetts 02139, USA*

(*Electronic mail: Andrzej.Janutka@pwr.edu.pl)

(Dated: 31 January 2024)

Performing micromagnetic simulations, we study the efficiency of response of bulk and polycrystalline nickel oxide (NiO) to high-frequency (up to 100GHz) magnetic fields with relevance to potential application of the antiferromagnet as a core material to high-frequency coils and resonators. NiO is advantageous due to its insulating property and high Neel temperature. Though the dynamical susceptibility of the antiferromagnet is low, the achievable product of susceptibility and frequency ("performance factor") appears to be relatively high, comparable to that of previously considered superferromagnetic systems. This makes NiO a potential core material for operating at extremely-high (sub-THz) frequency. The influence of thermal fluctuations on the susceptibility is estimated to be weak up to room temperature even for a nanocrystalline antiferromagnet, whereas, the magnetic response is linear for much wider ranges of frequencies and field amplitudes than for ferromagnetic and superferromagnetic systems.

I. INTRODUCTION

Antiferromagnets (AFs) have zero magnetostatic field and their magnetic resonance is in the THz range. Next to THz spintronic applications[1,2], interest in an enhanced sub-THz and THz magnetic response is related to chip-to-chip or to-chip wireless power transfer (WPT). Operating at sub-THz range allows for miniaturization of WPT systems relative to RF-based systems[3,4]. In the THz WPT area, much attention has been focused on controlling radiation via metamaterial based devices (superlenses and shields)[5–7]. With relevance to designing metamaterials, coupling split-ring resonators to AFs has been investigated[8,9]. A technique of efficient non-radiative transmission called magnetic coupling resonant WPT (MCR-WPT) uses inductive coils coupled to the transmitter and to the receiver[10]. The efficiency of MCR-WPT can be additionally improved via including magnetic cores into the coils[11]. At certain levels of miniaturization, the core material has to operate at a sub-THz range of frequencies, which draws our attention to AFs. We also consider the concept of converting electrical power on-chip using magnetic-core inductors or transformers. The smaller the device the higher the operating frequency has to be in order to compensate for the small value of the magnetic flux. Typically the GHz frequency of the ferromagnetic resonance provides a frequency limitation on use of the ferromagnets or ferromagnet-based composites as core materials. For AFs, the ultimate frequency is shifted up to sub-THz.

Operating ferromagnetic materials at high frequency leads to a fast increase of the eddy-current loss with frequency, which led to the interest in resistive superferromagnets and superparagnets for use as core materials[12–15]. In AFs, domain wall motion is not driven by an external field and AFs are insulators in the Mott phase. As well as having high electrical resistivity, AFs are advantageous because of their low hysteresis area, thus, low hysteresis loss. The aim of the present paper is numerical determination of the magnetic response of an insulating AF to a sub-THz frequency field of a relatively-high amplitude, thus, verification of its applicability as core material. Although, the total magnetic moment of AFs is zero and inducing significant magnetization requires the application of a high field, operating with several orders of magnitude higher frequency than is usual for ferromagnetic cores can possibly compensate for the lower induced magnetization by enabling a high inductive voltage.

In particular, we consider nickel mono-oxide, a widely studied AF whose major advantage is its high Neel temperature (well above the room temperature) $T_N = 523$K. An AF core could possibly be made of macroscopic crystals or of nanocrystals. In the first case, the antiferromagnetic-domain structure is determined by crystal defects (disclocations) which are accompanied by AF domain walls[16]. Thus, the domain structure of NiO is durable against the magnetic field application. On the other hand, considering nanocrystalline AF cores, we note that the nanocrystals of NiO can be monodomain AF particles provided they are sufficiently large to neglect some reordering at the nanocrystal surface[17]. Because of the strong inter-sublattice exchange, the energy of the inter-sublattice exchange of such nanocrystals is much higher than thermal energy. Thus, unlike for nanosized ferromagnets, thermal fluctuation effect on the antiferromagnetism in nanocrystals is expected to be suppressed. Also, the energy of the single-ion anisotropy in AF NiO is high compared to thermal energy. Therefore, we propose a common description of the magnetic response from monocrystalline and nanocrystalline NiO, treating the AF domains as separate magnetic particles.

The major characteristics determining the efficiency of magnetic materials in terms of the ability of inducing the electromotive force (for energy-conversion applications) is the product of frequency and the response-function amplitude called "performance factor"[18]. Due to very strong fields of the single-ion anisotropy and of the inter-sublattice exchange, the magnetic response of AFs is linear in a wide range of

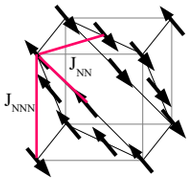

FIG. 1. The single cell of NiO crystal with connections between the nearest and next nearest neighbors indicated with red lines.

amplitude of the driving-field and the performance factor is well determined. Based on our previous analysis of efficiency of the response of MNP systems to high-frequency magnetic fields[19,20], we perform a comparison of achievable performance factors, showing values obtainable for NiO to be relatively high, thus, claiming AFs to be of potential interest with regard to the on-chip conversion of power.

The micromagnetic model of NiO-like AF is formulated in Sec. II and the results of its application to driven magnetization oscillations of NiO are presented and summarized in Sec. III.

II. MODEL

Consider a single AF domain or AF particle. Let us denote the sublattice magnetization vectors by $\boldsymbol{M}_1 = M\boldsymbol{m}_1$, $\boldsymbol{M}_2 = M\boldsymbol{m}_2$, where $M = M(T)$ and $|\boldsymbol{m}_1| = |\boldsymbol{m}_2| = 1$. The temperature dependence of the sublattice magnetization is taken in the form[21] $M(T) = M_0\,(1+T/2T_N)\sqrt{1-T/T_N}$, with $M_0 =$ 550kA/m. Also, let us define (renormalized) magnetization $\boldsymbol{m} \equiv (\boldsymbol{m}_1+\boldsymbol{m}_2)/2$ and Neel vector $\boldsymbol{l} \equiv (\boldsymbol{m}_1-\boldsymbol{m}_2)/2$. The macroscopic model of two-sublattice AF relevant to a series of fcc-lattice oxides like NiO and MnO is based on the Hamiltonian density of magnetic subsystem $\mathscr{H} = \mathscr{H}_{ex}+\mathscr{H}_{an}+\mathscr{H}_Z$;

$$\mathscr{H}_{ex} = A_1|\boldsymbol{m}|^2 + A_2\sum_{i=1}^{3}\left|\frac{\partial \boldsymbol{l}}{\partial x_i}\right|^2 = \frac{A_1}{2}(1+\boldsymbol{m}_1\cdot\boldsymbol{m}_2) + \frac{A_2}{4}\sum_{i=1}^{3}\left(\left|\frac{\partial \boldsymbol{m}_1}{\partial x_i}\right|^2 + \left|\frac{\partial \boldsymbol{m}_2}{\partial x_i}\right|^2 - 2\frac{\partial \boldsymbol{m}_1}{\partial x_i}\frac{\partial \boldsymbol{m}_2}{\partial x_i}\right), \quad (1)$$

$$\mathscr{H}_{an} = K_1\left[(\boldsymbol{m}_1\cdot\boldsymbol{n})^2+(\boldsymbol{m}_2\cdot\boldsymbol{n})^2\right] + K_2\left[\prod_{i=1}^{3}(\boldsymbol{m}_1\cdot\boldsymbol{n}_i)^2 + \prod_{i=1}^{3}(\boldsymbol{m}_2\cdot\boldsymbol{n}_i)^2\right], \qquad \mathscr{H}_Z = -2M\boldsymbol{m}\cdot\boldsymbol{B}.$$

Here $\boldsymbol{B}$ denotes an external field. The normal to the easy plane $\boldsymbol{n}$ is one of the set $(1,1,1)/\sqrt{3}$, $(-1,1,1)/\sqrt{3}$, $(1,-1,1)/\sqrt{3}$, $(1,1,-1)/\sqrt{3}$. The three easy directions $\boldsymbol{n}_1$, $\boldsymbol{n}_2$, $\boldsymbol{n}_3$ lie in the easy plane and they deviate from each other by an angle of 120^o.

In the effective fields on the sublattices

$$\boldsymbol{B}_{eff;1(2)} \equiv -\frac{\delta\mathscr{H}}{M\delta\boldsymbol{m}_{1(2)}} \equiv \boldsymbol{B}^{ex}_{eff;1(2)} + \boldsymbol{B}^{an}_{eff;1(2)} + \boldsymbol{B}, \quad (2)$$

the exchange parts take the form

$$\boldsymbol{B}^{ex}_{eff;1(2)} = \frac{4A_h}{M}\boldsymbol{m}_{2(1)} + \frac{2A_i}{M}\Delta\boldsymbol{m}_{1(2)} + \frac{A_{nhi}}{M}\Delta\boldsymbol{m}_{2(1)}, \quad (3)$$

where constants $A_h = -A_1/8$, $A_i = A_2/4$, $A_{nhi} = -A_2/2$ are written according to the notation of the BORIS package applied for micromagnetic simulations[22]. Macroscopic (micromagnetic) parameters for NiO are established based on the microscopic Hamiltonian $\hat{\mathscr{H}} = \hat{\mathscr{H}}_{ex}+\hat{\mathscr{H}}_{an}+\hat{\mathscr{H}}_Z$;

$$\hat{\mathscr{H}}_{ex} = J_{NN}\sum_{\langle j,\delta_j\rangle}\hat{\boldsymbol{s}}_j\cdot\hat{\boldsymbol{s}}_{j+\delta_j} + J_{NNN}\sum_{\langle j,\delta'_j\rangle}\hat{\boldsymbol{s}}_j\cdot\hat{\boldsymbol{s}}_{j+\delta'_j},$$

$$\hat{\mathscr{H}}_{an} = D_1\sum_j(\hat{\boldsymbol{s}}_j\cdot\boldsymbol{n})^2 + D_2\sum_j(\hat{\boldsymbol{s}}_j\cdot\boldsymbol{n}_1)^2(\hat{\boldsymbol{s}}_j\cdot\boldsymbol{n}_2)^2(\hat{\boldsymbol{s}}_j\cdot\boldsymbol{n}_3)^2,$$

$$\hat{\mathscr{H}}_Z = -M\delta V\sum_j\hat{\boldsymbol{s}}_j\cdot\boldsymbol{B}. \quad (4)$$

Here, $J_{NN} = -22\cdot10^{-23}$J and $J_{NNN} = 305\cdot10^{-23}$J are the nearest-neighbor (NN) and next-nearest-neighbor (NNN) exchange integrals[23], while the single-ion anisotropy constants are given by $D_1 = -38\mu$eV and $D_2 = 320$neV,[24], where δV denotes the volume per magnetic ion. The single cell of NiO crystal is visualized in Fig. 1. The numbers of NNs of a given spin which belong the same sublattice is 6 and it is equal to the number of its NN in the second sublattice. The number of NNNs of a given spin is 6 and they belong to another sublattice[25,26]. The energy of AF exchange interactions between NNNs dominate over the NN interaction energy and the comparison of microscopic Hamiltonian (upon approximating spin with classical vectors) to the macroscopic Hamiltonian leads us to the estimations

$$\frac{A_1}{2} = -4A_h = \frac{6J_{NN}}{(a/\sqrt{2})^3} + \frac{6J_{NNN}}{a^3} \approx 25\cdot10^7\,\mathrm{J/m^3},$$

$$\frac{A_2}{2} = -A_{nhi} = 2A_i = \frac{6J_{NN}}{a/\sqrt{2}} + \frac{6J_{NNN}}{a} \approx 4.4\cdot10^{-11}\,\mathrm{J/m}. \quad (5)$$

In a similar way, we compare the quantum and classical anisotropy Hamiltonians and we evaluate $K_{1(2)} = 2D_{1(2)}/a^3$. It should be noted that the spin anisotropy constants for NiO or related Mott insulators is a mixture of magnetic and magneto-elastic contributions. At high frequencies and high amplitude of the sublattice magnetization oscillations (due to a strong driving field), the magneto-elastic coupling induces dynamical strain which is not relaxing during oscillation cycles. Therefore, the effective magnetic anisotropy model relevant to fast dynamics is different than the one considered for the slow dynamics description, for instance, the description of domain wall creation and domain-wall motion[27]. While, the latter requires dealing with simultaneous evolution of the magnetic and elastic degrees of freedom, in the former, the magnetic evolution is studied separately via averaging the lattice oscillations.

In order to implementint the model to the micromagnetic (BORIS) package, it is important to express the anisotropy energy using only three constant vectors and a little algebra leads us to

$$\mathscr{H}_{an} = 2K_1 - \frac{2}{3}K_1\sum_{i=1}^{3}\left[(\boldsymbol{m}_1\cdot\boldsymbol{n}_i)^2+(\boldsymbol{m}_2\cdot\boldsymbol{n}_i)^2\right] + K_2\left[\prod_{i=1}^{3}(\boldsymbol{m}_1\cdot\boldsymbol{n}_i)^2 + \prod_{i=1}^{3}(\boldsymbol{m}_2\cdot\boldsymbol{n}_i)^2\right]. \quad (6)$$

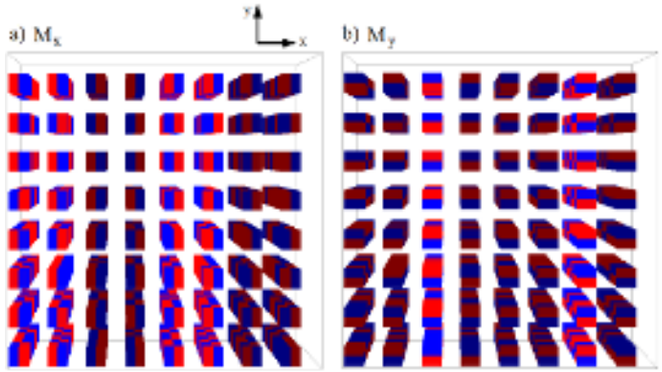

FIG. 2. Spatial distribution of magnetization components of the simulated system of single-domain particles, which are treated as isolated computational cells. Color intensities (from red to blue) correspond to the projection of macrospin of the (a) left or right and (b) upper or lower sublattices onto x-axis and y-axis, correspondingly.

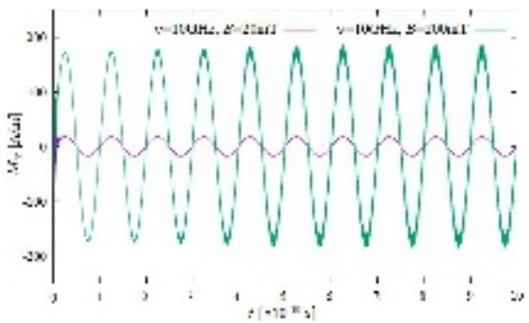

FIG. 3. Time dependence of magnetization component parallel to the linearly-polarized driving field of amplitude 20mT (purple line) and 200mT (green line) at frequency 10GHz.

Within the stochastic Landau-Lifshitz-Gilbert (sLLG) approach, thermal fluctuations can be included into the considerations of the AF dynamics. By analogy to superferromagnetic systems, thermal fluctuations in AF nanoparticles could be of especial importance for their magnetic response[28–30]. However, besides larger sizes of AF nanoparticles than achievable for ferromagnetic nanoparticles, another factor makes thermal fluctuations negligible. We show that, unlike for typical ferromagnetic nanoparticles, the thermal energy is low compared

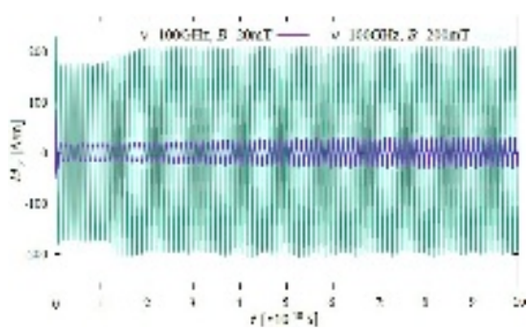

FIG. 4. Time dependence of magnetization component parallel to the linearly-polarized driving field of amplitude 20mT (purple line) and 200mT (green line) at frequency 100GHz.

to the exchange energy as well as to the magnetic anisotropy energy of AF nanocrystals of NiO. In particular, considering (for estimation purposes) as small AF nanocrystal of NiO as 5nm×5nm×5nm (denoting the particle volume with V), one finds characteristic switching temperatures $K_1 V/k_B = 1450$K and $4|A_h|V/k_B = 2.2 \cdot 10^6$K. In fact, real nanocrystals have to be be considerably larger to be considered as AFs (of sufficiently large volume to surface ratio), thus, their magnetic states are even better protected against thermal fluctuations[17]. The only macroscopic effect of temperature is its influence on the value of the sublattice magnetization[31,32].

The high value of the AF exchange field raises a problem when implementing micromagnetic code. One of the exchange lengths of AF is $l_{ex}^{AF} \equiv \sqrt{A_2/A_1} = \sqrt{-A_i/2A_h}$. For NiO, we establish $l_{ex}^{AF} = 0.42$nm, thus, the exchange length is equal to the lattice constant, which makes the micromagnetic approach to the ordering inhomogeneity invalid. The requirement of the summary sublattice macrospin of the computational cell to be high and the requirement of the cell edge not to be larger than the exchange length are contradictory. On the other hand, local inhomogeneities of the magnetization (which is zero except at lattice imperfections) are not expected to strongly influence the magnetic response of the AF system and we finally neglect them putting all the gradient terms in the macroscopic Hamiltonian as zero, $A_2 = 4A_i = -2A_{nhi} = 0$. Hence, we restrict the problem to homogeneous magnetization oscillations (AFMR) in a system of many AF nanocrystals or domains in a bulk AF. According to this simplification, any domain or nanocrystal is represented in simulations as a single computational cell. Let us emphasize that we simulate AF below the frequency of the spin-wave gap.

Measurements of the Gilbert damping constant for NiO have been reported in[31]. They indicate the damping constant to be very low $\sim 10^{-4}$. Taking into account possible structure imperfections (especially present in polycrystalline materials), following[24], we perform numerical simulations for the damping constant of $\alpha = 0.005$ which is a much higher value than reported for perfect NiO, while, being relatively small compared to those of metallic ferromagnets.

III. RESULTS AND CONCLUSION

We generate a number of isolated cubic cells and, for each cell, we draw one of four possible easy planes. For a given sublattice-plane direction, the axes of in-plane anisotropy are uniquely determined by the cell corners. The relaxed magnetization state is visualized in Fig. 2. We simulate numerically the application of a linearly-polarized driving field $\boldsymbol{B}(t) = [0, B\sin(2\pi\nu t), 0]$ to the system of many single-cell domains. The longitudinal (with respect to the driving field) component of the magnetization $M_y = M_{1y} + M_{2y}$ (the response function) is plotted in Figs. 3 and 4 as function of time. The amplitude of oscillations of M_y it found to be a linear function of the field amplitude B in a reasonably-wide range of the field (we considered $B = 20\text{mT} \div 200\text{mT}$), for the frequencies of 10GHz and 100GHz. Also, we do not find any noticeable phase shift of the response function relative to the

driving field for these frequencies, (100GHz is one order of magnitude lower than the frequency of AFMR[33]), which is desirable with respect to avoiding hysteresis loss.

Following Figs. 3 and 4, we evaluate the susceptibility $\chi = \mu_0 \mathrm{Amp}(M_y)/B(= 0.22\mathrm{mT}/200\mathrm{mT}) = 1.1 \cdot 10^{-3}$, where $\mathrm{Amp}(M_y)$ denotes the amplitude of the response function. Though this value is low, it is constant up to the frequency of 100GHz and almost constant up to room temperature[32,34]. Thus, achievable performance factor takes the value $\nu \cdot \chi = 1.1 \cdot 10^8 \mathrm{s}^{-1}$ at least. It is comparable to that predicted for a superparamagnetic system with susceptibility $\chi \sim 1$ at the driving-field amplitude $B = 20\mathrm{mT}$ which can be efficiently operated at the frequencies up to $\nu \sim 0.1\mathrm{GHz}$, however, beyond the linear response regime[20].

Besides driving with a simple linearly-polarized AC field, we have tested the application of a rotating field to driving the AF system. For similar values of the frequency and field amplitude, we obtained almost the same amplitudes of the response function as for the driving with both the linearly-polarized and rotating fields, unlike for ferromagnetic and superferromagnetic systems[19]. Also, we have tested additional application of a DC field perpendicular to the driving (linear or rotating) field, which is a way of influencing the magnetic response in superparamagnetic systems, according to Ref.[20]. This way also did not appear to be efficient in terms of increasing the amplitude of the response function of NiO.

Summarizing, we state that the predicted response of an AF insulator to a sub-THz field is relevant to spintronic and power transfer applications of these materials. This is due to its high performance factor and the natural insulating property present without any structural engineering.

ACKNOWLEDGEMENTS

The authors acknowledge support of a MISTI-Poland award from MIT.

REFERENCES

[1] V. Baltz, A. Manchon, M. Tsoi, T. Moriyama, T. Ono, Y. Tserkovnyak, Antiferromagnetic spintronics, Rev. Mod. Phys. **90**(1), 015005 (2018).
[2] T. Jungwirth, J. Sinova, A. Manchon, X. Marti, J. Wunderlich, C. Felser, The multiple directions of antiferromagnetic spintronics, Nature Phys. **14**, 200—203 (2018).
[3] Hanh Dang-ba, Gyung-su Byun, A Sub-THz Wireless Power Transfer for Non-Contact Wafer-Level Testing, Electronics **9**(8), 1210 (2020).
[4] N. Shinohara, Trends in Wireless Power Transfer: WPT Technology for Energy Harvesting, Mllimeter-Wave/THz Rectennas, MIMO-WPT, and Advances in Near-Field WPT Applications, IEEE Microwave Mag. **22**(1), 46–59 (2021).
[5] T. J. Yen *et al.*, Terahertz Magnetic Response from Artificial Materials, Science **303**(5663), 1494–1496 (2004).
[6] C. Rong *et al.*, A critical review of metamaterial in wireless power transfer system, IET Power Electron. **14**(9), 1541—1559 (2021).
[7] J. Zhou, P. Zhang, J. Han, L. Li, Y. Huang, Metamaterials and Metasurfaces for Wireless Power Transfer and Energy Harvesting, Proc. IEEE **110**(1), 31–55 (2022).
[8] Y. Mukai, H. Hirori, T. Yamamoto, H. Kageyama, K. Tanaka, Nonlinear magnetization dynamics of antiferromagnetic spin resonance induced by intense terahertz magnetic field, New J. Phys. **18**(1), 013045 (2016).
[9] D. M. Heligman, R. V. Aguilar, Numerical Simulation of the Coupling between Split-Ring Resonators and Antiferromagnetic Magnons, https://arxiv.org/abs/2109.05086.
[10] A. Kurs, A. Karalis, R. Moffatt, J. D. Joannopoulos, P. Fisher, M. Soljacic, Wireless Power Transfer via Strongly Coupled Magnetic Resonances, Science **317**(5834), 83–86 (2007).
[11] D. Wang *et al.*, Modern Advances in Magnetic Materials of Wireless Power Transfer Systems: A Review and New Perspective, Nanomaterials **12**(20), 3662 (2022).
[12] C. R. Sullivan, D. V. Harburg, J. Qiu, C. G. Levey, D. Yao, Integrating magnetics for on-chip power: a perspective, IEEE Trans. Power Electron. **28**(9), 4342–4353 (2013).
[13] R. J. Kaplar, J. C. Neely, D. L. Huber, L. J. Rashkin, Generation-after-next power electronics: ultrawide-bandgap devices, high-temperature packaging, and magnetic nanocomposite materials, IEEE Power Electron. Mag. **4**(1), 36–42 (2017).
[14] D Hasegawa, H. Yang, T. Ogawa, M. Takahashi, Challenge of ultra high frequency limit of permeability for magnetic nanoparticle assembly with organic polymer—Application of superparamagnetism, J. Magn. Magn. Mat. **321**, 746–749 (2009).
[15] M. Kin, H. Kura, T. Ogawa, Core loss and magnetic susceptibility of superparamagnetic Fe nanoparticle assembly, AIP Adv. **6**(12), 125013 (2016).
[16] N. B. Weber, H. Ohldag, H. Gomonaj and F. U. Hillebrecht, Magnetostrictive Domain Walls in Antiferromagnetic NiO, Phys. Rev. Lett. **91**(23), 237205 (2003).
[17] A. C. Gandhi, H.-Y. Cheng, Y.-M. Chang and J. G. Lin, Size confined magnetic phase in NiO nanoparticles, Mater. Res. Express **3**(3), 035017 (2016).
[18] A. J. Hanson, J. A. Belk, S. Lim, C. R. Sullivan, D. J. Perreault, Measurements and performance factor comparisons of magnetic materials at high frequency, IEEE Trans. Power Electr. **31**(11), 7909–7925 (2016).
[19] K. Brzuszek, A. Janutka, High-frequency magnetic response of superferromagnetic nanocomposites, J. Magn. Magn. Mat. **543**, 168608 (2022).
[20] K. Brzuszek, C. A. Ross, A. Janutka, High-frequency magnetic response of superparamagnetic composites of spherical $Fe_{65}Co_{35}$ nanoparticles, J. Magn. Magn. Mat. **573**, 170651 (2023).
[21] V. Barsan and V. Kuncser, Exact and approximate analytical solutions of Weiss equation of ferromagnetism and their experimental relevance, Phil. Mag. Lett. **97**(9), 359—371 (2017).
[22] http://www.boris-spintronics.uk/
[23] M. T. Hutchings and E. J. Samuelsen, Measurement of spin-wave dispersion in NiO by inelastic neutron scattering and its relation fo magnetic properties, Phys. Rev. B **6**(9), 3447–3461 (1972).
[24] T. Chirac, J.-Y. Chauleau, P. Thibaudeau, O Gomonay and M. Viret, Ultrafast antiferromagnetic switching in NiO induced by spin transfer torques, Phys. Rev. B **102**(13), 134415 (2020).
[25] I. V. Solovyev, Exchange interactions and magnetic force theorem, Phys. Rev. B **103**(10), 104428 (2021).
[26] M. Hafez-Torbati, F. B. Anders and G. S. Uhrig, Simplified approach to the magnetic blue shift of Mott gaps, Phys. Rev. B **106**(20), 205117 (2022).
[27] O Gomonay and D Bossini, Linear and nonlinear spin dynamics in multidomain magnetoelastic antiferromagnets, J. Phys. D: Appl. Phys. **54**(37), 374004 (2021).
[28] B. Ouari, S. Aktaou and Y. P. Kalmykov, Reversal time of the magnetization of antiferromagnetic nanoparticles, Phys. Rev. B **81**(2), 024412 (2010).
[29] Yu L Raikher and V I Stepanov, Magneto-orientational behavior of a suspension of antiferromagnetic particles, J. Phys.: Condens. Matter **20**(20), 204120 (2008).
[30] I. S. Poperechny and Y. L. Raikher, Low-frequency dynamic magnetic susceptibility of antiferromagnetic nanoparticles with superparamagnetic properties, Magnetism **2**(4), 340—355 (2022).
[31] T. Moriyama, K. Hayashi, K. Yamada, M. Shima, Y. Ohya, T. Ono, Intrinsic and extrinsic antiferromagnetic damping in NiO, Phys. Rev. Materials **3**(5), 051402(R) (2019).
[32] S. Thota, J. H. Shim, M. S. Seehra, Size-dependent shifts of the Néel temperature and optical band-gap in NiO nanoparticles, J. Appl. Phys. **114**(21), 214307 (2013).

[33]Y. Shoji, E. Ohmichi, H. Takahashi and H. Ohta, Antiferromagnetic resonance spectroscopy of NiO in the terahertz region, 2022 47th International Conference on Infrared, Millimeter and Terahertz Waves (IRMMW-THz), Delft, Netherlands, 2022, pp. 1–2.

[34]G. Srinivasan, M. S. Seehra, Magnetic susceptibilities, their temperature variation, and exchange constants of NiO, Phys. Rev. B **29**(11), 6295 (1984).